

Design, synthesis, and biological testing of potential heme-coordinating nitric oxide synthase inhibitors

Elizabeth A. Litzinger,^{a,b} Pavel Martásek,^c Linda J. Roman^c and Richard B. Silverman^{a,b,*}

^aDepartment of Chemistry, The Center for Drug Discovery and Chemical Biology, Northwestern University, Evanston, IL 60208-3113, USA

^bDepartment of Biochemistry, Molecular Biology, and Cell Biology, The Center for Drug Discovery and Chemical Biology, Northwestern University, Evanston, IL 60208-3113, USA

^cDepartment of Biochemistry, University of Texas Health Science Center, San Antonio, TX 78384-7760, USA

Received 23 November 2005; accepted 16 December 2005

Available online 20 January 2006

Abstract—Based on computer modeling of the active site of nitric oxide synthases (NOS), a series of 10 amidine compounds (**9–18**) was designed including potential inhibitors that involve the coordination of side-chain functional groups with the iron of the heme cofactor. The most potent and selective compound was the methylthio amidine analogue **9**, which was more potent than L-nitroarginine with 185-fold selectivity for inhibition of neuronal NOS over endothelial NOS. It also exhibited time-dependent inhibition, but did not involve the mechanism previously proposed for other amidine inhibitors of NOS. None of the compounds, however, exhibited heme-binding characteristics according to absorption spectroscopy.

© 2005 Elsevier Ltd. All rights reserved.

1. Introduction

The conversion of L-arginine to L-citrulline and nitric oxide (NO) is catalyzed by nitric oxide synthase (NOS). NO is an important secondary biological messenger¹ that mediates many important processes, such as the immune response,² blood regulation,³ and neuronal signaling.⁴ However, overproduction of NO has been implicated in several disease states, such as neurodegenerative diseases,⁵ strokes,⁶ and rheumatoid arthritis.⁷

Since attenuation of NO may favorably affect the diseases mentioned above, potent NOS inhibitors are constantly being sought. Most of the early compounds were based on L-arginine, the NOS substrate (Fig. 1). Instead of the unsubstituted terminal guanidine nitrogen, the inhibitors shown contain either a substituted terminal guanidine nitrogen or replacement of the terminal nitrogen with another functional group. In large part, these are competitive inhibitors that maintain key ligand–receptor interactions: amino acid contacts in the

L-configuration and hydrogen bonding between the ligand and a glutamate residue in the active site. In an effort to develop more potent NOS inhibitors, possible contacts with the enzyme other than hydrogen bonds were explored. An inhibitor that could bind as an iron ligand to the active site heme seemed like a reasonable approach. L-Thiocitrulline (**5**), an arginine analogue with the terminal guanidine-nitrogen replaced by sulfur, has been reported to have a $K_i = 0.06 \pm 0.01 \mu\text{M}$ against rat nNOS and to coordinate to the iron as the sixth ligand via the thiourido sulfur.⁸ However, absorption spectroscopy revealed a ‘modified’ Type II difference spectrum. In comparison to a known iron-coordinating ligand such as imidazole, with a peak at 432 nm and a trough at 393 nm, L-thiocitrulline displayed a peak at 435 nm, a shoulder at 413 nm, and a trough at 393 nm. The authors suggested that this arose because the sulfur atom in the active site is not correctly aligned with the iron and reaches a statistical equilibrium between positioning itself as the sixth ligand and being too far away to perturb the d electron orbitals. Indeed, inspection of the crystal structure obtained by Crane et al.⁹ of L-thiocitrulline shows a distance of about 4.0 Å between the sulfur atom and iron, considerably longer than that reported for axial Fe–S distances of about 2.30 Å in analogous cytochrome P-450 model systems.¹⁰

Keywords: Nitric oxide synthase; Nitric oxide synthase inhibition; Heme-binders; Heme ligands; Enzyme inhibition; Enzyme inactivation; Absorption difference spectra.

*Corresponding author. Tel.: +1 847 491 5653; fax: +1 847 491 7713; e-mail: Agman@chem.northwestern.edu

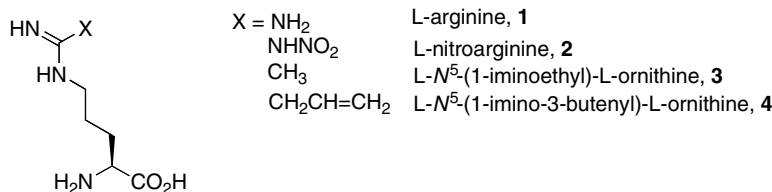
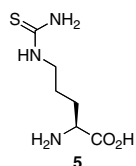
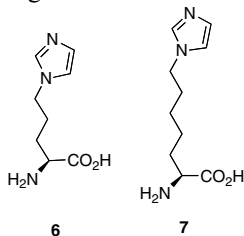


Figure 1. NOS substrate arginine and inhibitors.



Other NOS inhibitors have also been reported as heme-coordinating ligands. Imidazole attached to amino acid functional groups via a backbone of three and five methylenes (**6** and **7**, respectively) were found to be potent nNOS inhibitors with $K_i = 2 \mu\text{M}$ for each.¹¹ This was a great improvement upon imidazole itself, with an $\text{IC}_{50} = 200 \mu\text{M}$,¹² presumably the result of additional enzyme contacts facilitated by the amino acid. Difference absorption spectroscopy elicited a Type-II spectrum, indicative of iron ligation.



We hypothesized that the potency could be further increased by incorporating key features of L-thiocitrulline and compounds **6** and **7** into a new class of inhibitors. A guanidine moiety, missing from **6** and **7** but mimicked by the nitrogens of the thiourea group of L-thiocitrulline, was known to be necessary for strong binding to NOS.¹³ To allow the heme-coordinating ligand to have the mobility to reach closer to the heme iron, a flexible tether was attached to the ligand rather than attaching it directly to the guanidine group. Computer modeling of the guanidine analogues shown in **Figure 2** and the corresponding amidines indicated that the amidines would be more effective. This series of compounds was synthesized; the results of these studies are described here.

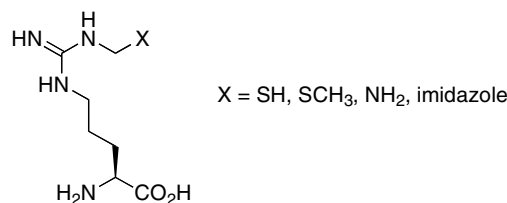


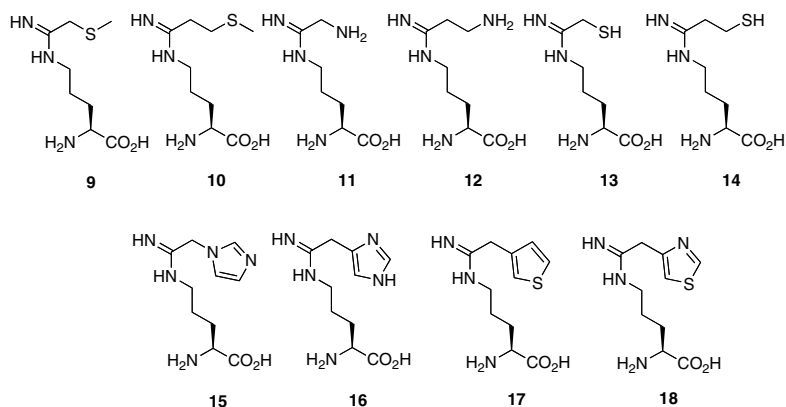
Figure 2. Initially proposed heme-binding inhibitors of NOS.

2. Results

2.1. Computer modeling

The basic scaffold shown in **Figure 2** was tested using the FlexX docking program in Sybyl software, version 6.8.¹⁴ Initial attempts to dock **8** as an iron ligand in the active site were unsuccessful, as placement of the guanidino nitrogen directly above the iron prevented the sulfur from accessing it. The structure was then modified to the amidine (**9**). Substitution of the nitrogen with a flexible carbon arm allowed the sulfur to move closer to the heme and coordinate to the iron (**Fig. 3**).

In addition to **9**, structures **10–18** also were modeled into the active site. These compounds included common ligands such as sulfide, amino, thiol, imidazole, thiophene, and thiazole. Thiophene has been shown to substitute as the thiolate ligand in cytochrome P-450 model systems;¹⁵ thiazole has been found to coordinate to eNOS.¹⁶ Along with positioning the molecule within the active site, FlexX evaluated the binding energies of the ligands to the enzyme for the 30 most favorable docked positions in the nNOS active site. The energy of the most favorable conformation for each structure is listed in **Table 1**, with L-nitroarginine used as a reference.



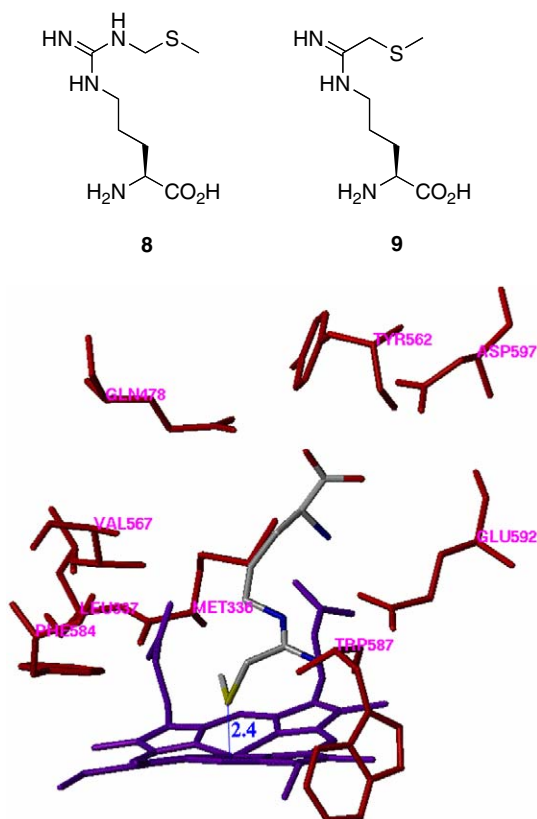


Figure 3. Predicted conformation of **9** in the NOS active site. The sulfur atom is 2.4 Å from the heme iron, as indicated by the line.

Table 1. Binding energies of substituted amidines from FlexX evaluations

9	$n = 1, X = \text{SCH}_3$	14	$n = 2, X = \text{SH}$
10	$n = 2, X = \text{SCH}_3$	15	$n = 1, X = 1\text{-imidazole}$
11	$n = 1, X = \text{NH}_2$	16	$n = 1, X = 4\text{-imidazole}$
12	$n = 2, X = \text{NH}_2$	17	$n = 1, X = 4\text{-thiophene}$
13	$n = 1, X = \text{SH}$	18	$n = 1, X = 4\text{-thiazole}$
Compound	E_{docked} (kJ/mol)		
L-NA	−22.06		
9	−24.30		
10	−10.26		
11	−33.26		
12	−34.24		
13	−20.51		
14	−19.37		
15	−21.94		
16	−27.83		
17	−22.22		
18	−21.41		

Compound **10** had a much higher binding energy than all of the other compounds. Based on simulated docking, the longer alkyl chain prevented the amidine from

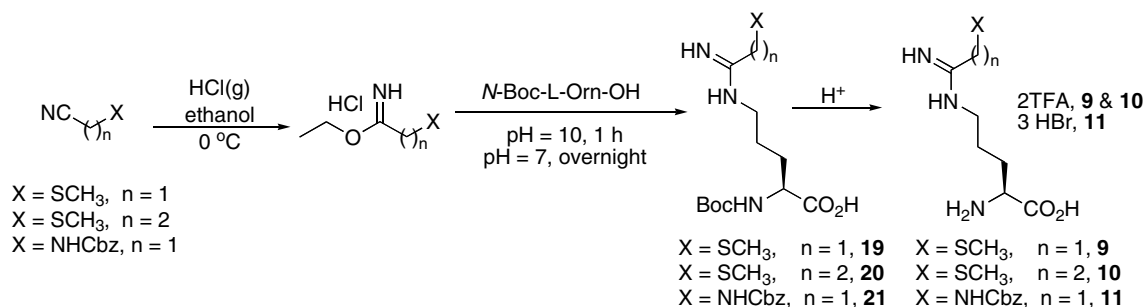
interacting with the glutamate residue. Some predicted conformations of **11** and **12** showed the terminal amino group interacting with the peptidyl backbone instead of the heme, but all would result in highly potent compounds. The thiol analogues of **9** and **10** also were tested. Although **13** was predicted to interact with the heme, **14** was forecasted to bind in a hydrophobic pocket. 1-Imidazole-containing **15** was depicted in three different positions: parallel to the heme porphyrin, coordinating to the heme porphyrin, and outside of the active site entirely with the amino acid portion in the heme binding pocket. An imidazole attached at the 4-position to the amino acid scaffold (**16**) also was included to see if additional contacts afforded by the 1-nitrogen could increase potency. Structure **16** was predominantly shown parallel to the heme with additional contacts to the peptidyl backbone forming the heme cavity. Most conformations of **17** were shown with the thiophene parallel to the heme, but **18** was shown both perpendicular to the heme for coordination and parallel to it. As with **15**, **16–18** also were predicted to have several conformations with the structure inverted in the active site. None of these, however, were calculated to have significantly lower binding energies. Structures **9–18** represent the final compounds synthesized. Although it was predicted to bind poorly, **10** was included to investigate the predictive capabilities of the FlexX docking program.

2.2. Chemistry

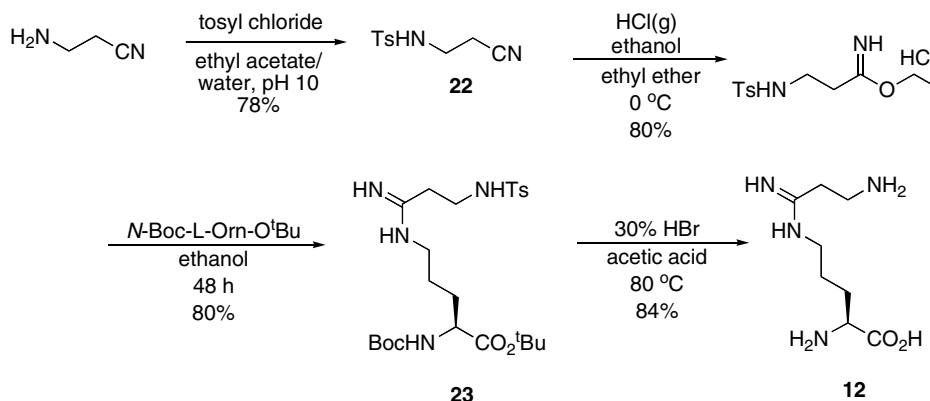
The basic synthetic plan for all of the inhibitors involved the use of an imidic ester as the amidine precursor, itself generated from a nitrile (Scheme 1). In the case of aminoacetonitrile, the amino group was protected as a carbamate. This, along with the methylthio ether-containing nitriles, was converted to the corresponding ethyl imidic esters using standard Pinner synthesis conditions.¹⁷ The imidates were used directly to generate the amidines using conditions previously reported,¹⁸ and the resulting amidines were purified by cation-exchange chromatography. In all cases, the amidine was selectively displaced from the ion-exchange resin with an aqueous pyridine solution. Final Boc deprotection using either trifluoroacetic acid (TFA) in methylene chloride for compounds **9** and **10** or hydrogen bromide in acetic acid for **11** completed the synthesis.

For the amine-containing compound **12**, 3-aminopropionitrile was protected with a tosyl group (Scheme 2). The resulting compound **22** and its imidic ester did not dissolve readily in water, and coupling was instead completed with *N*^α-Boc-L-Orn-O^tBu in ethanol. Removal of all three protecting groups was accomplished with hydrogen bromide in acetic acid at 80 °C. Proton NMR spectra of both final amine-containing compounds showed evidence of intramolecular bonding, as concluded from splitting patterns observed with the C^δ- and C^ω-hydrogens.

The thiol-containing compounds were synthesized using procedures modified from previous literature



Scheme 1.



Scheme 2.

precedent. Many methods were attempted to create **13**; however, none was successful without concomitant oxidation of the thiol group. Compound **14** was made from the symmetrical disulfide **24**. As a result of poor solubility of the diimidic ester in water, amidine coupling was completed with *N*^α-Boc-L-Orn-O^tBu in ethanol (Scheme 3). The disulfide was reduced with triphenylphosphine, then the Boc and *tert*-butyl ester groups were removed simultaneously with acid. In contrast to **13**, purification of **14** did not lead to thiol oxidation. As with the amino-containing inhibitors, proton NMR spectroscopy gave evidence of intramolecular hydrogen bonding.

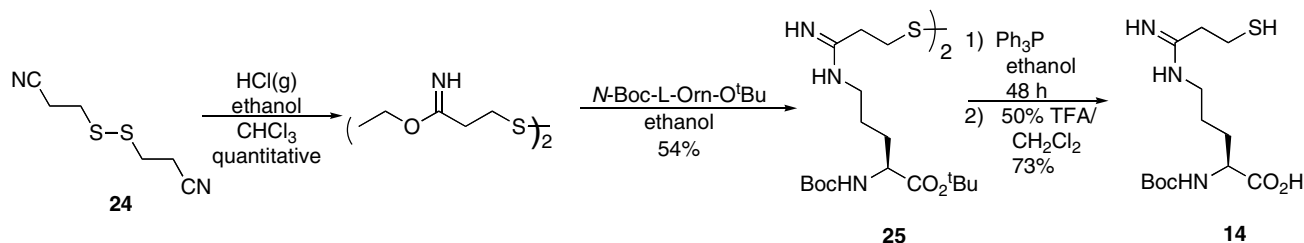
The potential heterocyclic inhibitors were synthesized using the same basic synthetic scheme previously used (Scheme 4). This was used directly for compounds **16** and **17**; formation of 1-methylcyanoimidazole (**26**) from bromoacetonitrile and imidazole was first carried out before continuing with the amidine synthesis for **27**. Acidic deprotection of the Boc group using conventional conditions of initially proposed 4-thiazole-containing **18** unfortunately led to hydrolysis of the thiazole moiety. To circumvent the problem of heterocycle decomposition, the thiazole was substituted at the C-2 position with a methyl group.¹⁹ Based on computer modeling, it appeared that the NOS active site could accommodate the methyl group, even in the position required for thiazole coordination. To test this, the synthesis shown in Scheme 5 was carried out. Ethyl 2-methylthiazole-4-carboxylate was reduced to the alcohol (**30**), converted to the chloride, and substituted with cyanide (**31**), from which the imidic methyl

ester was made. Coupling with *N*-Boc-L-ornithine to **32**, purification, and deprotection with hydrochloric acid gave **33**.

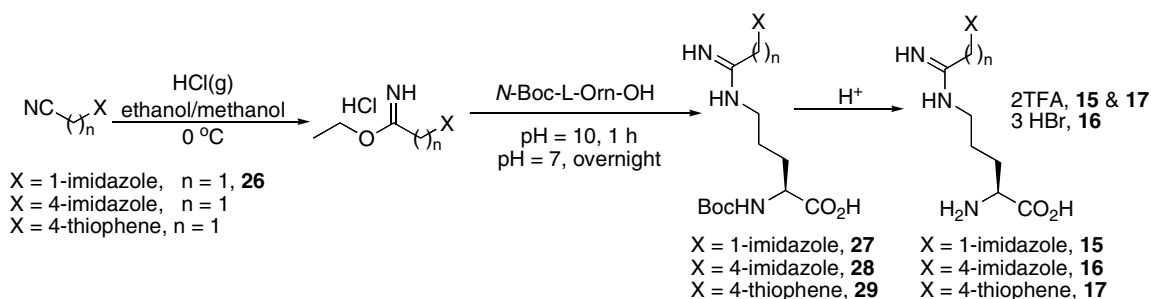
2.3. Biological results

The compounds were tested against all three isoforms of NOS, and IC₅₀ values were obtained for each (Table 2). L-Nitroarginine was included for comparison. Although most compounds showed poor inhibition, **9** showed relatively good potency and selectivity for nNOS. Compounds **11** and **12**, although less potent than **9**, also showed selectivity for nNOS. Compound **14** had potency similar to that of L-nitroarginine for iNOS, but was less potent against the other isoforms. K_i values were determined from Dixon plots for **9** and **14** for each isozyme, along with L-nitroarginine (Table 3). Based on these assays, **9** had comparable potency toward nNOS as L-nitroarginine but was 260 times (185/0.71) more selective for nNOS over eNOS than L-nitroarginine. Selectivity over iNOS was minimal (3-fold), as in the case of L-nitroarginine. Inhibitor **14** was 4-fold less potent than L-nitroarginine against iNOS, but was twice as selective for nNOS over iNOS than L-nitroarginine.

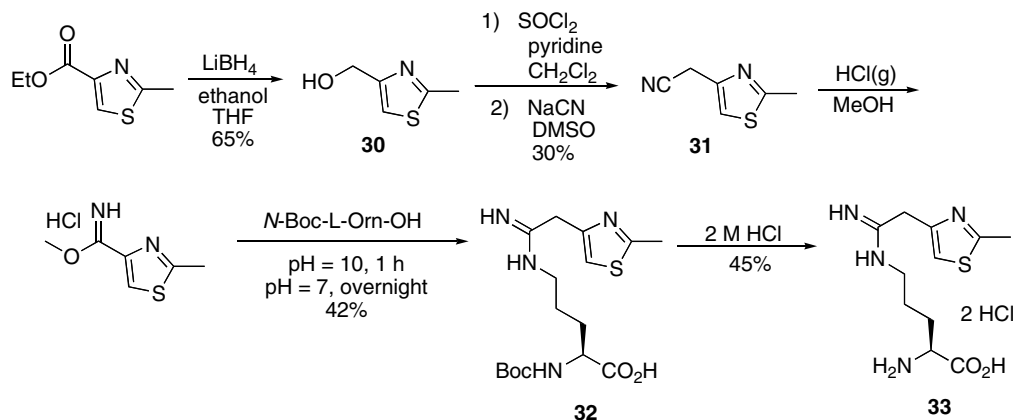
Compounds **9–12** and **14** were tested for ligand–iron coordination by absorption spectroscopy. The spectra for **9** and for imidazole, which is known to bind to the NOS heme, are shown in Figure 4. Representative of all new compounds tested, they show a peak at about 400 nm and a trough at 437 nm (Type I spectrum), in comparison to bound imidazole with a trough at



Scheme 3.



Scheme 4.



Scheme 5.

403 nm and a peak at 440 nm (Type II spectrum). All five compounds gave Type I spectra when inhibitor was added to nNOS saturated with imidazole, indicative of pentacoordinate high-spin heme iron. Therefore, it appears that the inhibitors do not interact with the heme iron.

In addition to initial velocity inhibition, **9** and **14** were also tested for time-dependent inactivation. Compound **9** demonstrated time- and concentration-dependent inactivation of nNOS in the presence of NADPH. No inactivation was observed in the presence of excess L-arginine or NADP⁺. Kinetic constants for inactivation were $K_I = 74.32 \mu\text{M}$ and $k_{\text{inact}} = 0.11 \text{ min}^{-1}$ as determined by a Kitz and Wilson replot of the inactivation data.

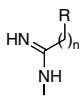
Compound **14** was screened for inactivation of iNOS at 0 °C. At this temperature, no inactivation was seen. A second inactivation screening, this time at 37 °C, showed inactivation of iNOS both with and without NADPH in

the incubation mixture. No inactivation was seen when 1.5 mM L-arginine was added to the incubation mixture. In both cases, inactivation was concentration dependent. From the incubation mixture containing NADPH, K_I and k_{inact} values of $92.28 \mu\text{M}$ and 0.29 min^{-1} were calculated. Assays conducted with **14** and nNOS at 0 °C also showed no inactivation.

Compound **9** was tested for irreversibility of inactivation. After inactivation, incubation mixtures as previously prepared were diluted with substrate at a concentration 10-fold higher than that of **9**. After monitoring every 10 min for 1 h, no increase in nNOS activity was seen in the incubation containing **9**; no decrease was observed in the control.

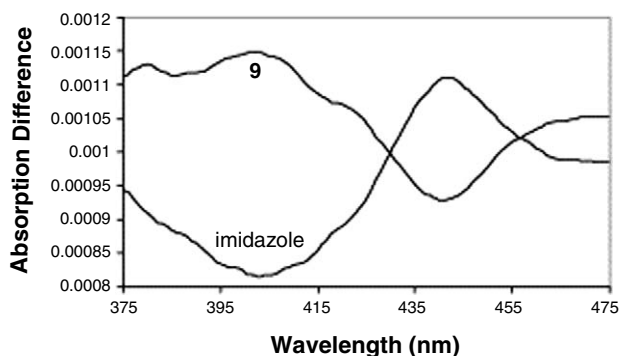
The formation of biliverdin IX α as a result of inactivation of iNOS by **9** was monitored by HPLC. Biliverdin IX α is a known heme degradation product formed by other amidine-containing inactivators.^{18a,20} Incubation mixtures without (Fig. 5B) and with **9** (Fig. 5C) were

Table 2. IC₅₀ values for inhibitors against all three NOS isoforms^a

		<i>n</i>	IC ₅₀ (μM)		
R			nNOS	iNOS	eNOS
L-Nitroarginine	NHNO ₂	0	4.736	8.70	3.84
9	SCH ₃	1	8.57	14.75	186.92
10	SCH ₃	2	74.66	39.78	235.39
11	NH ₂	1	36.06	51.07	120.86
12	NH ₂	2	76.16	79% ^a	85% ^a
14	SH	2	85.88	17.33	60.89
15	1-Imidazole	1	43% ^a	92 ^a	>95% ^a
16	4-Imidazole	1	67% ^a	63% ^a	>95% ^a
17	4-Thiophene	1	81% ^a	88% ^a	>95% ^a
33	4-(2-Methyl)-thiazole	1	41% ^a	75% ^a	69% ^a

^a Percent enzyme activity with 300 μM compound present.**Table 3.** Table of *K_i* values and selectivity for **9** and **14**

	<i>K_i</i> (μM)			<i>n/i</i>	<i>n/e</i>
	nNOS	iNOS	eNOS		
L-Nitroarginine	0.55	1.44	0.39	2.63	0.71
9	0.37	1.17	68.7	3.12	185
14	33.3	5.67	51.0	5.87	1.54

Selectivity given as the reciprocal of the nNOS/iNOS or nNOS/eNOS *K_i* ratio.**Figure 4.** Difference absorption spectra for **9** and imidazole.

examined when enzyme was initially added (time = 0) and after activity was no longer observed in the mixture containing **9** (time = 4.5 h). The control experiment developed no biliverdin peak over time, and the heme peak remained consistent in area (Fig. 5B). Likewise, the incubation containing **9** did not develop a peak corresponding to biliverdin, even after the enzyme was fully

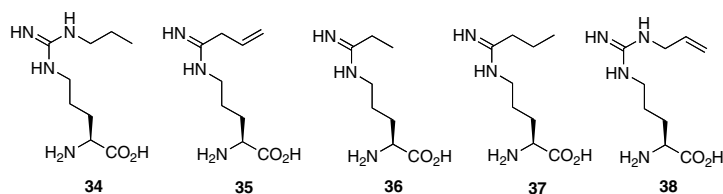
inactivated (Fig. 5C). Further, the change in area of the heme peak between the two chromatographs was only 1.3%. A standard curve using known quantities of biliverdin IX α indicated that it would have been detected at the concentrations of the experiment if it were produced.

3. Discussion

A series of amidine-containing inhibitors designed to coordinate to the NOS heme iron were first examined using the FlexX docking program. Structures synthesized according to computer modeling were expected to have equal or superior potency to that of L-nitroarginine, the inhibitor used as a standard for comparison. Only one structure, **9**, actually exhibited potency slightly better than that of L-nitroarginine for nNOS; compound **14** was only slightly less potent than L-nitroarginine against iNOS. The others demonstrated considerably lower potency for all three isoforms. Compound **9** was the most potent and selective inhibitor of nNOS synthesized, with an experimentally determined *K_i* = 0.37 μM and a selectivity ratio of 185 for nNOS/eNOS. However, difference absorption spectra exhibited a Type I spectrum when added to imidazole-saturated nNOS. This indicates that the sulfur-containing chain does not interact with the heme iron and probably preferentially binds in the hydrophobic pocket at the top of the active site.

The selectivity for nNOS over eNOS displayed by **9** had previously been observed with other guanidine- and amidine-containing inhibitors related to L-arginine, including *N*^ω-propyl-L-arginine²¹ (**34**) and *N*⁵-(1-imino-3-butenyl)-L-ornithine²² (**35**); **34** has a reported selectivity of 149 for nNOS/eNOS, while that for **35** is 120. Therefore, **9** has slightly greater selectivity than those inhibitors. However, **34** and **35** displayed great selectivity for nNOS versus iNOS: **34** has a 3158-fold selectivity and **35** 600-fold selectivity. The selectivity of **9** for nNOS over iNOS was only 3-fold. In this respect, **9** is similar to *N*⁵-(1-iminopropyl)-L-ornithine (**36**) and *N*⁵-(1-iminobutyl)-L-ornithine (**37**).²² These compounds showed only a 3- and 2-fold preference for nNOS over iNOS and 3- and 3.3-fold selectivities for nNOS over eNOS, respectively.

It is interesting that **9** shows greater selectivity for nNOS over eNOS but not over iNOS. Structurally, compound **9** most resembles **37**, which would lead to the prediction that no isoform selectivity would be seen. It is unclear how **9** differentiates between isoforms, but it is apparent that the hydrophobic and larger sulfur atom is impor-



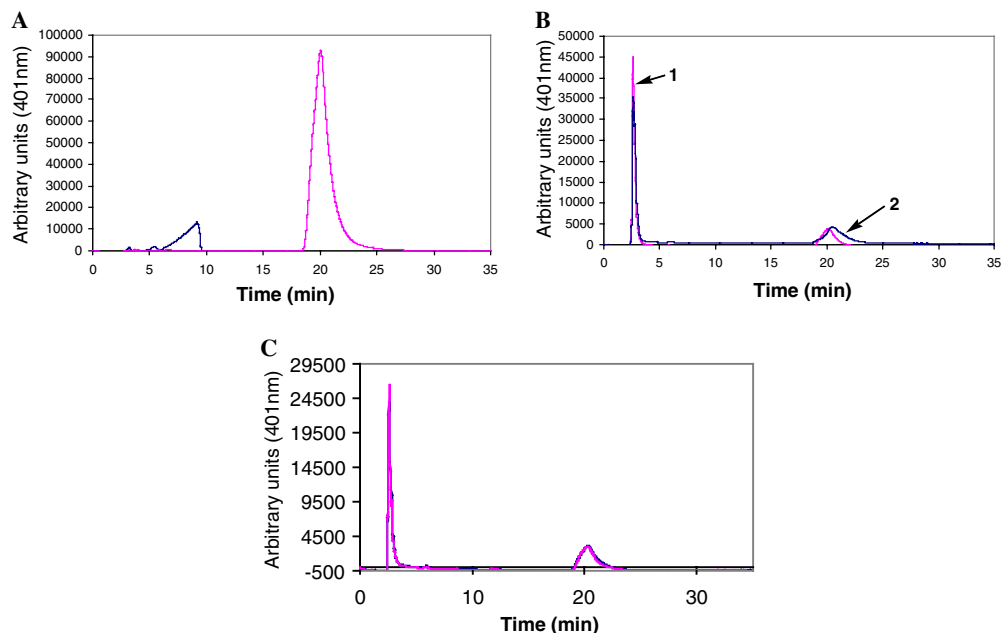


Figure 5. HPLC chromatograms following inactivation of iNOS by **9**. (A) Hemin and biliverdin IX α standards. (B) Incubation without **9** at time = 0 (**1**) and 4.5 h (**2**). (C) Incubation with **9** at time = 0 and 4.5 h (virtually no difference).

tant. Whereas the unsaturated bond in **35** seems to be important for selectivity between nNOS and the other isoforms as compared to **37**, *N*^ω-allyl-L-arginine (**38**) shows only 10.5-fold and 15.5-fold selectivities for nNOS over iNOS and eNOS, respectively, compared to the much larger nNOS selectivity for the saturated compound **34**.²³ It seems that neither hydrocarbon chain length nor unsaturation alone can account for selectivity. It is possible that the bulkier, more polarizable sulfur may fit in the hydrophobic pocket differently than saturated or unsaturated hydrocarbon chains, which in turn leads to a different selectivity trend among isoforms. Crystal structures of the above-mentioned compounds, including **9**, bound to the isoforms may elucidate these trends further.

Not only have **34** and **35** been reported as selective inhibitors, but they also show NADPH-dependent inactivation. Compound **9** was found to be a concentration-, time-, and NADPH-dependent inactivator of nNOS. Inactivation appeared to be irreversible, as addition of L-arginine at a concentration 10 times that of **9** restored no activity after one hour. Initial inactivation-control experiments showed that L-arginine in the inactivation mixture from the start prevented inactivation, most likely by preventing **9** from accessing the active site. The inability of L-arginine to restore activity was suggestive of some type of modification of nNOS by **9**. It was hypothesized that the mechanism of inactivation was similar to that of *N*⁵-(1-iminoethyl)-L-ornithine (**3**), the mechanism of which has previously been studied.^{18a} This inactivator oxidizes the active site heme to biliverdin IX α , using electrons supplied from NADPH. HPLC chromatography of **9**-inactivated iNOS, however, showed no peak corresponding to biliverdin IX α in the inactivation mixture after 4.5 h. According to a standard curve constructed from chromatographs of biliverdin IX α at varying concentrations, the degradation product would have

been detectable with the amount of enzyme used. Additionally, the area under the heme peak decreased by only 1.3% after inactivation by **9**. nNOS inactivators, including **3**, **34**, and **38**, have all produced considerable decrease in the heme absorption at 401 nm as a result of heme modification.^{18a,23} Although both **3** and **9** contain amidines in close proximity to the heme, the HPLC data suggest a different mechanism of inactivation. Studies beyond the scope of this work would be required to determine the inactivation mechanism of **9**.

Inhibitor **10**, the two-methylene carbon analogue of **9**, was synthesized and screened as a test of the docking simulation. Modeling results gave a binding energy substantially lower than that of L-nitroarginine or any of the other compounds. The computer model showed that the ligand was not fully positioned within the active site; the longer chain prevented the cationic amidine from reaching the glutamate residue important for binding. This prediction proved to be correct, as the IC₅₀ value for **10** was 18-fold higher than that for L-nitroarginine.

The computer modeling of structures **11** and **12** showed the terminal amino group in an extended conformation, interacting with either the iron or engaged in hydrogen bonds with the peptidyl backbone of the active site. In both cases, the potency was predicted to be greater than that of L-nitroarginine. Both compounds were synthesized, but on final protecting group removal, hydrogen bonding between the amino and amidine groups was observed by NMR spectroscopy, suggesting a different conformation was favored resulting from the intramolecular hydrogen bonding. Compounds **11** and **12**, therefore, were not very potent, with IC₅₀ values against nNOS approximately nine and 19 times greater, respectively, than that of L-nitroarginine. This relatively hydrophilic moiety

may have interacted unfavorably with the known hydrophobic pocket in the active site.²⁴

It was thought that mercaptan **14** would mimic the methylthiol compounds (**9** and **10**) by coordinating to the heme iron, but even more tightly. Inhibitor **14**, however, proved to be only a moderately potent inhibitor, with a K_i value of 5.67 μM against iNOS with some selectivity over eNOS (9-fold) but less so over nNOS (6-fold). It was surprising that **14**, which has a chain extending away from the amidine containing the same number of atoms as **9**, was not more selective for nNOS over iNOS and eNOS. As with compounds **11** and **12**, **14** gave evidence of intramolecular hydrogen bonding by proton NMR spectroscopy. This constraint may have prevented the usual selectivity pattern seen with longer-chain alkyl arginines and amidines, which would prevent the sulfhydryl group from interacting with the iron, in agreement with the Type I difference spectrum that was recorded for **14** against both nNOS and iNOS.

Compound **14** was also tested for inactivation. At 0 °C, no inactivation was observed for either iNOS or nNOS over the typical experiment time of 40 min at concentrations between 100 and 200 μM . At 37 °C, iNOS was inactivated in the presence of NADPH and NADP⁺. This did not allow for the definitive assignment of non-NADPH-dependent inactivation; rather, remnant reducing agents from the enzyme preparation may have been present in the incubation mixture.

Heterocycle-containing compounds **15–17** and **33** were very poor inhibitors, all having IC_{50} values equal to or greater than 300 μM . This was surprising, considering that the computer-calculated binding energies for these structures were similar to that of L-nitroarginine; imidazole-containing compound **16** was lower than that for L-nitroarginine. The ligand was predicted to bind in three different ways: (1) inserted into the active site with the amidine interacting with the glutamate and the imidazole coordinating to iron; (2) inserted into the active site with the imidazole parallel to the heme porphyrin; and (3) with the molecule inverted, the amino acid in the heme pocket and the imidazole blocking the active site channel. In all cases, binding was predicted to be better than that of L-nitroarginine, but this was not observed. Possibly, the molecules do not gain access to the heme site or do not fit well once there. As seen with the previous alkyl amidines, the amidine group provides enough interaction to display at least some competitive inhibition.

4. Summary

A series of nNOS inhibitors intended to coordinate to the active site heme iron were designed and evaluated using a computer ligand-docking program, synthesized, and tested. These compounds contained an amidine spaced by at least one methylene carbon to an iron-coordinating moiety to allow the moiety access to the iron without perturbing the important amidine–glutamate interaction. Two of these compounds, methylthiol-containing **9** and **10**, had potencies as predicted. The

amino-containing compounds **11** and **12**, and the mercaptan **14** exhibited unexpected intramolecular hydrogen binding that changed the conformation of the molecules and gave lower inhibition than predicted. Compounds containing a heterocycle, either imidazole (**15**, **16**), thiophene (**17**), or thiazole (**33**), were extremely poor inhibitors despite the predictions of the docking program for several successful binding modes.

Most surprising was the fact that none of the compounds functioned as a heme ligand, as evidenced by their difference absorption spectra. For compounds **11**, **12**, and **14**, the intramolecular binding may have prevented the terminal moiety from reaching the iron. Compound **9** showed considerable selectivity for nNOS and iNOS over eNOS, but not because of heme coordination. The cavity size is isoform-dependent, with nNOS being the largest, followed by eNOS and iNOS.²⁵ Therefore, it was surprising that **9** would favor nNOS and iNOS over eNOS. Possibly the sulfur-containing chain produced enough steric hindrance to discriminate between nNOS and eNOS.

Finally, **9** displayed concentration-, time-, and NADPH-dependent irreversible inactivation. The mechanism of inactivation is not the same as other amidines previously reported.^{18a,20}

5. Experimental

5.1. Computer docking simulations

The molecular modeling was performed using SYBYL 6.8 software (Tripos) on a Silicon Graphics Octane2 workstation. Each inhibitor was constructed and optimized by the molecular mechanics method with the Tripos force field. The charge was calculated by the Gasteiger–Marsili method. Molecular docking was performed using the FlexX3.0 program. The optimized structure was used as the starting conformation for docking. L-Nitroarginine was used as a reference for insertion into the L-nitroarginine /nNOS crystal structure complex. Of the 30 conformations returned per inhibitor, the lowest binding energy is reported.

5.2. Materials

All common organic solvents were purchased from Fisher Scientific. All deuterated solvents were purchased from Cambridge Isotope Laboratories. Amino acid derivatives were obtained from EMD Biosciences. Tetrahydrobiopterin (H_4B) was purchased from Alexis Biochemicals. Billiverdin IX α was obtained from ICN Biomedicals, Inc. All other chemicals were purchased from Aldrich, unless otherwise noted.

5.3. Analytical methods

¹H NMR spectra were recorded on a Varian spectrometer of specified frequency. Chemical shifts are reported as δ values in ppm from TMS (δ 0.00) as the internal

standard in CDCl₃. For samples run in D₂O, the HOD resonance was set at 4.80 ppm. For samples run in CD₃OD, the CD₃OH resonance was set at 4.87 ppm. High-resolution spectra were obtained on a Micromass 70-VSE instrument at the Mass Spectroscopy Laboratory of the University of Illinois at Urbana-Champaign. Thin-layer chromatography (TLC) was carried out on E. Merck pre-coated silica gel 60 F₂₅₄ plates and visualized with a ninhydrin spray reagent or iodine. Standard silica gel 60 from Sorbent Technologies was used for flash chromatography. For samples purified by HPLC, a Beckman System Gold (Model 125P solvent module and Model 166 detector) was used in conjunction with a Phenomenex Luna C₁₈ semi-prep column. Samples were eluted using a ratio of 95% solvent A (0.5% TFA in water) to 5% solvent B (0.5% TFA in acetonitrile) for 15 min, then changing to 90% solvent A over 15 min at a flow rate of 1.70 mL/min.

5.4. Syntheses

5.4.1. *N*¹-Boc-*N*⁵-(1-Imino-2-(methylthio)ethyl)-L-ornithine (19). A three-necked flask that had been flame-dried and placed under argon was charged with (methylthio)acetonitrile (5.00 mL, 59.62 mmol) and reagent-grade, anhydrous ethanol 3.47 mL (59.50 mmol). The solution was cooled to 0 °C, and then HCl gas was bubbled through for 1 h. The reaction was stirred for another 4 h on ice and then left to come to room temperature overnight with stirring. The next morning nitrogen was blown over the mixture to evaporate the solvent to dry the imidic ethyl ester to give 3.41 g (2.02 mmol, 34%) of slightly off-white solid that was used in the next step without purification. ¹H NMR (300 MHz, DMSO) δ 12.70 (br s, 1H), 11.35 (br s, 1H), 4.89 (q, *J* = 6.6 Hz, 2H), 4.09 (s, 2H), 2.60 (s, 3H), 1.72 (t, 7.0 Hz, 3H).

N^α-Boc-L-Orn(Cbz)-OH (0.80 g, 2.18 mmol) was hydrogenated overnight in 15 mL methanol using Pd/C as catalyst to remove the Cbz-protecting group. The product was filtered through Celite and concentrated to give 0.61 g (2.14 mmol, 98%) of the free amine, which was dissolved in water (12 mL), and 2.5 M NaOH was added until pH paper turned blue (pH ≥ 10). The imidic ester (0.60 g, 3.53 mmol) was added slowly while maintaining basic pH with additional sodium hydroxide solution. Once the addition was complete, the solution was allowed to stir at room temperature for 1 h, after which time it was neutralized with 1 M HCl and allowed to stir overnight. The next day amidine formation was evaluated by TLC (7:3 methanol/pyridine, *R*_f = 0.66). The column was purified by ion-exchange chromatography (Bio-Rad 50X, H⁺, 200–400 mesh) and eluted with 3% aqueous pyridine. Compound **19** was obtained as an off-white solid in 34% yield (0.23 g, 0.73 mmol). ¹H NMR (500 MHz, D₂O) δ 3.93 (m, 1H), 3.52 (s, 2H), 3.36 (t, *J* = 6.0 Hz, 2H), 2.13 (s, 3H), 1.83–1.70 (m, 4H), 1.43 (s, 9H). HRMS (ESI) (*m/z*): M+H⁺ calcd for C₁₃H₂₆N₃O₄S 320.1644, found 320.1654.

5.4.2. *N*¹-Boc-*N*⁵-(1-Imino-3-(methylthio)propyl)-L-ornithine (20). Compound **20** was synthesized following the

same procedure as **19**. 3-Methylmercaptopropionitrile was obtained from Karl Industries. The ethyl imidic ester was made in a 52% yield (5.02 g, 27.43 mmol) and used in the next step without further purification. ¹H NMR (300 MHz, DMSO) δ 12.45 (br s, 1H), 11.50 (br s, 1H), 4.62 (q, *J* = 7.2 Hz, 2H), 3.16 (t, *J* = 6.9, 2H), 2.98 (t, *J* = 6.9 Hz, 2H), 2.27 (s, 3H), 1.52 (t, *J* = 7.2 Hz, 3H).

N^α-Boc-L-Orn-OH (2.03 g, 8.75 mmol) was allowed to react with the above imidic ester (4.10 g, 22.50 mmol) using the same procedure as **19** to yield **20** (1.22 g, 3.67 mmol, 42%). ¹H NMR (500 MHz, D₂O) δ 3.94 (m, 1H), 3.32 (m, 2H), 2.87 (m, 2H), 2.79 (m, 2H), 2.15 (s, 3H), 1.85–1.70 (m, 4H). HRMS (ESI) (*m/z*): M+H⁺ calcd for C₁₄H₂₈N₃O₄S 334.1801, found 334.1792.

5.4.3. *N*¹-Boc-*N*⁵-(1-Imino-2-*N*-Cbz-aminoethyl)-L-ornithine (21). *N*-Cbz-aminoacetonitrile (1.51 g, 7.94 mmol) and ethanol (3 mL, 51.10 mmol) were used as described above to prepare 1.89 g (6.94 mmol, 88%) of the imidic ester that was used without further purification. ¹H NMR (300 MHz, DMSO) δ 12.65 (br s, 1H), 11.60 (br s, 1H), 8.07 (br s, 1H), 7.35 (s, 5H), 5.07 (s, 2H), 4.48 (t, *J* = 6.4 Hz, 2H), 4.15 (d, *J* = 7.5 Hz, 2H), 1.31 (t, *J* = 6.3 Hz, 3H).

N^α-Boc-L-Orn-OH (0.59 g, 2.54 mmol) was dissolved in water (8 mL) and the solution made basic with 2.5 M NaOH. All of the imidic ester generated in the previous step was added to the solution, with just enough methanol added to maintain solubility of the ester. One hour later the solution was neutralized with 2 M HCl and let stir overnight. The next day methanol was removed in vacuo, and the resulting aqueous solution was loaded directly onto the ion-exchange resin (Bio-Rad 50X, H⁺, 200–400 mesh) and eluted with a 5% aqueous pyridine solution to yield 0.19 g (0.46 mmol, 18%) of **21** as a light yellow solid. ¹H NMR (500 MHz, CD₃OD) δ 7.36 (m, 5H), 5.13 (s, 1H), 3.96 (m, 1H), 3.03 (s, 2H), 2.93 (t, *J* = 5.5 Hz, 2H), 1.83–1.69 (m, 4H), 1.43 (s, 9H). HRMS (ESI) (*m/z*): M+H⁺ calcd for C₂₀H₃₁N₄O₆ 423.2235, found 423.2244.

5.4.4. *N*⁵-(1-Imino-2-(methylthio)ethyl)-L-ornithine (9). Compound **19** (0.55 g, 1.80 mmol) was dissolved in 50% TFA/CH₂Cl₂ (9 mL) and stirred for 1 h. Removal of solvent gave **9** in a 93% yield (0.37 g, 1.68 mmol) as a white solid. A portion of the product was further purified by HPLC. ¹H NMR (400 MHz, D₂O) δ 4.06 (t, *J* = 6.0 Hz, 1H), 3.51 (s, 2H), 3.40 (t, *J* = 7.2 Hz, 2H), 2.14 (s, 3H), 2.02 (m, 2H), 1.84 (m, 2H). HRMS (ESI) (*m/z*): M+H⁺ calcd for C₈H₁₈N₃O₂S 220.1120, found 220.1111. Anal. (C₈H₁₇N₃O₂S·2TFA·0.5H₂O) Calcd: C, 31.58; H, 4.42; N, 9.21; S, 7.01. Found: C, 31.55; H, 4.19; N, 8.93; S, 6.69.

5.4.5. *N*⁵-(1-Imino-3-(methylthio)propyl)-L-ornithine (10). Compound **20** (1.1 g, 3.31 mmol) was deprotected with 50% TFA/CH₂Cl₂ to yield 0.767 g (3.26 mmol, 98%) of the product as a light-yellow solid. A portion of the

product was further purified by HPLC. ^1H NMR (500 MHz, D_2O) δ 3.87 (m, 1H), 3.34 (t, J = 7.0 Hz, 2H), 2.85 (t, J = 6.5 Hz, 2H), 2.76 (t, J = 6.5 Hz, 2H), 2.13 (s, 3H), 1.95 (m, 2H), 1.82–1.73 (m, 2H). HRMS (ESI) (m/z): $\text{M}+\text{H}^+$ calcd for $\text{C}_8\text{H}_{18}\text{N}_3\text{O}_2\text{S}$ 234.1268, found 234.1276.

5.4.6. N^5 -(1-Imino-2-aminoethyl)-L-ornithine (11). Compound **21** (0.11 g, 0.26 mmol) was added to a 30% HBr/acetic acid solution (3 mL) under an argon atmosphere. The solid did not dissolve immediately and was left to stir overnight. The desired compound was precipitated out of solution upon the addition of cold diethyl ether (50 mL), filtered, and washed again with ether to give **11** in a quantitative yield (48.0 mg, 0.26 mmol) as a hygroscopic orange solid. A portion of the product was purified by HPLC. ^1H NMR (400 MHz, D_2O) δ 4.12 (t, J = 6.0 Hz, 1H), 4.10 (s, 2H), 3.43 (t, J = 6.8 Hz, 2H), 3.06 (t, J = 7.2 Hz, 1H), 2.10–1.78 (m, 4H), 1.95 (m, 2H), 1.82–1.73 (m, 2H). HRMS (ESI) (m/z): $\text{M}+\text{H}^+$ calcd for $\text{C}_7\text{H}_{17}\text{N}_4\text{O}_2$ 189.2275, found 189.2376.

5.4.7. 3- N -(p -Ts)-Aminopropionitrile (22). In accordance with the procedure of Rapoport and co-workers,²⁶ 3-aminopropionitrile fumarate (1.31 g, 12.57 mmol) was dissolved in water (14 mL). The solution was adjusted to pH 10 with 1 M NaOH and then tosyl chloride (2.66 g, 13.96 mmol) in ethyl acetate (6 mL) was added. After being stirred overnight, the layers were separated, and the aqueous layer was neutralized with 1 M HCl and extracted with ethyl acetate. The organic layer was dried over MgSO_4 and the solvent was removed in vacuo. The product was recrystallized from ethanol/water to give 2.19 g (78%) of **22**. ^1H NMR (500 MHz, CDCl_3) δ 7.76 (d, J = 8.1 Hz, 2H), 7.34 (d, J = 8.0 Hz, 2H), 5.07 (br s, 1H), 3.26 (q, J = 6.6, 2H), 2.59 (t, J = 6.6, 2H), 2.45 (s, 3H). HRMS (ESI) (m/z): $\text{M}+\text{H}^+$ calcd for $\text{C}_{10}\text{H}_{12}\text{N}_2\text{O}_6\text{S}$ 225.0698, found 225.0702.

5.4.8. N^1 -Boc- N^5 -(1-Imino-3- N -(p -Ts)-aminopropyl)-L-ornithine *tert*-butyl ester (23). Compound **22** (0.55 g, 6.90 mmol) was added to anhydrous, reagent-grade ethanol (7.0 mL, 120.03 mmol) and 1M HCl/ethyl ether (12 mL) and then chilled at 0 °C. Once all of the **22** had dissolved, HCl gas was bubbled through the solution for 1 h and then left to stir another 5 h at 0 °C. The reaction mixture was stored at 4 °C overnight without stirring. After this time, ethyl ether was added to precipitate the product, which was filtered and washed again with ether and dried to give the imidic ester (1.70 g, 5.54 mmol, 80%), which was used in the next step without further purification. ^1H NMR (400 MHz, DMSO) δ 12.45 (br s, 1H), 11.25 (br s, 1H), 8.09 (t, J = 6.4 Hz, 1H), 7.79 (d, J = 8.0 Hz, 2H), 7.53 (d, J = 7.6 Hz, 2H), 4.46 (q, J = 7.6 Hz, 2H), 3.16 (q, J = 6.0 MHz, 2H), 2.86 (t, J = 6.80 MHz, 2H), 2.62 (s, 3H), 1.44 (t, J = 7.2 Hz, 3H).

N^α -Boc-L-Orn(Z)-OH was converted to the *tert*-butyl ester by the method of Takeda et al.²⁷ Briefly, N^α -Boc-L-Orn(Z)-OH (1 g, 2.73 mmol) was stirred for 2 h with

1.6 equiv of di-*tert*-butyl dicarbonate (0.96 g, 7.33 mmol) and 0.3 equiv of 4-(dimethylamino)pyridine (DMAP, 0.10 g, 0.82 mmol) in *tert*-butanol (10 mL). The solvent was removed in vacuo, and the DMAP was removed by eluting the residue through a short silica column with 4:1 hexanes/ethyl acetate to obtain the ester in a 93% yield (1.10 g, 2.53 mmol). Hydrogenation of the benzyl carbamate as described before gave N^α -Boc-L-Orn-O t Bu that was used immediately.

The di-protected ornithine (1.30 g, 4.53 mmol) was dissolved in anhydrous methanol (12.5 mL), and the imidic ester (0.47 g, 1.57 mmol) was added. The solution was left to stir at room temperature for 48 h, after which time cold diethyl ether (100 mL) was added and the solution was chilled at 4 °C overnight. The next day a brown oil was retrieved from the sides of the flask, which was dried in vacuo to give **23** (0.63 g, 1.23 mmol, 80%). ^1H NMR (500 MHz, CD_3OD) δ 7.76 (d, J = 5.5 Hz, 2H), 7.28 (d, J = 5.5 Hz, 2H), 4.1 (m, 1H), 3.33 (m, 2H), 2.98 (m, 2H), 2.43 (t, J = 6.4 Hz, 2H), 2.35 (s, 3H), 1.78–1.64 (m, 4H), 1.45 (s, 9H), 1.41 (s, 9H). HRMS (ESI) (m/z): $\text{M}+\text{H}^+$ calcd for $\text{C}_{24}\text{H}_{41}\text{N}_4\text{O}_6\text{S}$ 513.2747, found 513.2756.

5.4.9. N^5 -(1-Imino-3-aminopropyl)-L-ornithine (12). Into a pressure tube that had been flame-dried and cooled under vacuum were added phenol (1.00 g, 10.64 mmol), **23** (0.19 g, 0.37 mmol), and a minimal amount (<1 mL) of anhydrous methanol. Once the solids had dissolved, 30% HBr in acetic acid (10 mL) was added, and the tube was sealed and heated for 5 h at 85–90 °C. After cooling overnight, water (30 mL) was added, the solution cooled on ice, and then extracted with ethyl acetate until the aqueous layer was of a clear brown color; **12** (62 mg, 0.31 mmol, 84%) was obtained as a hygroscopic orange solid. A portion of the product was further purified by HPLC. ^1H NMR (400 MHz, D_2O) δ 4.12 (t, J = 6.0 Hz, 1H), 3.35 (t, J = 10.4 Hz, 2H), 3.04 (t, J = 7.8 Hz, 2H), 2.91 (t, J = 8.0, 2H), 2.02 (m, 2H), 1.82 (m, 2H). HRMS (ESI) (m/z): $\text{M}+\text{H}^+$ calcd for $\text{C}_8\text{H}_{19}\text{N}_4\text{O}_2$ 203.1508, found 203.1512.

5.4.10. 3,3'-Dithiobis(N -[*tert*-butyl N^4 -Boc-4-*S*-butanolate]propionamide) dihydrochloride (25). Diethyl 3,3'-dithiobis(propionimidate) dihydrochloride was synthesized from 3,3'-dithiobispropionitrile (1.53 g, 8.91 mmol) and ethanol (1.4 mL, 24.00 mmol) as described by Johnston and Gallagher²⁸ to give the disulfide product in a quantitative yield (3.00 g, 8.87 mmol), which was used in the next step without additional purification. ^1H NMR (400 MHz, D_2O) δ 4.45 (q, J = 7.2 Hz, 2H), 3.11–3.08 (m, 4H), 1.45 (t, J = 6.8 Hz, 3H).

N^α -Boc-L-Orn-O t Bu (1.11 g, 3.83 mmol), prepared as described above for **23**, was thoroughly dried and then dissolved in anhydrous ethanol (5 mL) under argon. To this was added the imidic ester (0.65 g, 1.93 mmol), and the resulting suspension was stirred for 72 h. Absolute ethanol (6 mL) was added, and the solution was stirred for 24 h more. At the end of this time, cold ethyl ether was added and the solution was

cooled to 4 °C for 5 h. The viscous yellow oil that collected at the bottom of the flask was separated from the liquid and dried to give **25** (1.28 g, 1.70 mmol, 89%) as a tacky yellow solid. ¹H NMR (300 MHz, CDCl₃) δ 5.76 (br s, 1H), 4.16 (br s, 4H), 3.88 (q, *J* = 6.9 Hz, 4H), 3.47 (m, 2H), 2.13–1.87 (m, 4H), 1.63 (d, *J* = 8.7 Hz, 9H), 1.38 (t, *J* = 7.2 Hz, 3H). HRMS (ESI) (*m/z*): M+H⁺ calcd for C₈H₁₉N₄O₂ 750.4130, found 750.4145.

5.4.11. N⁵-(1-Imino-3-mercaptopropyl)-L-ornithine (14). Compound **25** (0.50 g, 0.67 mmol) was dissolved in anhydrous ethanol (5 mL) and anhydrous THF (2 mL). To this was added triphenylphosphine (0.54 g, 2.01 mmol), and the solution was stirred for 72 h. As much solvent as possible was removed in vacuo, then 50% TFA/CH₂Cl₂ (6 mL) was added. The resulting solution was stirred for 1 h, the solvent was removed, the residue was dissolved in 2 M HCl (10 mL) and extracted with methylene chloride. The aqueous layer was concentrated to give **14** (0.26 g, 0.91 mmol, 73%). A portion of the product was further purified by HPLC. ¹H NMR (500 MHz, D₂O) δ 3.93 (t, *J* = 6.5 Hz, 1H), 3.35 (t, *J* = 7.0, 2H), 3.33 (s, 1H), 2.86 (t, *J* = 6.5 Hz, 2H), 2.76 (t, *J* = 6.5 Hz, 2H), 2.00–1.95 (m, 2H), 1.84–1.72 (m, 2H). HRMS (ESI) (*m/z*): M+H⁺ calcd for C₈H₁₈N₃O₂S 220.1120, found 220.1117.

5.4.12. 1-Cyanomethylimidazole (26). The synthesis of **26** was prepared as previously described.²⁹ Imidazole (4.03 g, 59.20 mmol) was charged to a flask that had been flame-dried and cooled under nitrogen. Freshly distilled THF (80 mL) was added, and once all of the imidazole had dissolved, sodium hydride (2.44 g, 61.10 mmol, 60% in mineral oil) was added portionwise as a solid. After hydrogen evolution had ceased, stirring was increased to a vigorous rate. Bromoacetonitrile (4.1 mL, 58.90 mmol) was added dropwise over 1.5 h. As the bromoacetonitrile was added, the opaque white solution gradually turned yellow, then orange in color. Stirring was continued for an additional 4.5 h, then the solution was concentrated and the residue was dissolved in water (50 mL) and extracted with methylene chloride. Purification by silica gel chromatography (100:7 CH₂Cl₂/methanol) gave **26** (4.44 g, 41.50 mmol, 70%) as a brown liquid. ¹H NMR (500 MHz, CDCl₃) δ 7.59 (s, 1H), 7.16 (s, 1H), 7.06 (s, 1H), 5.04 (s, 2H). HRMS (ESI) (*m/z*): M+H⁺ calcd for C₅H₆N₃ 108.0562, found 108.0549.

5.4.13. N¹-Boc-N⁵-(1-Imino-2-(1-imidazolyl)ethyl)-L-ornithine (27). To a flask that had been flame-dried and cooled under nitrogen was added **26** (2.11 g, 19.70 mmol), reagent-grade ethanol (2.0 mL, 34.30 mmol), and dry benzene (8 mL). The solution was cooled on ice and then HCl gas was bubbled through the solution for 50 min with vigorous stirring. Stirring was continued for another 2 h, at which time a brown precipitate collected at the bottom of the flask. The solvent was concentrated and the solid was dried to give the imidic ester (2.77 g, 14.73 mmol, 74%) as a light-brown solid, which was used in the next step without further purification. ¹H NMR (400 MHz, D₂O) δ 8.78

(s, 1H), 7.50 (s, 1H), 5.19 (s, 2H), 4.28 (q, *J* = 7.2 Hz, 2H), 1.27 (t, *J* = 7.2 Hz, 3H).

Coupling of the imidic ester (1.60 g, 8.47 mmol) with N^α-Boc-L-Orn-OH (0.77 g, 3.33 mmol) in the usual manner gave **27** (1.08 g, 3.19 mmol, 87%) after ion-exchange chromatography. ¹H NMR (500 MHz, D₂O) δ 8.70 (s, 1H), 7.46 (s, 2H), 4.86 (s, 2H), 3.92 (m, 1H), 3.02 (t, *J* = 5.6 Hz, 2H), 1.83–1.71 (m, 4H), 1.43 (s, 9H). HRMS (ESI) (*m/z*): M+H⁺ calcd for C₁₀H₁₈N₅O₂ 340.4102, found 340.4009.

5.4.14. N¹-Boc-N⁵-(1-Imino-2-(4-imidazolyl)-ethyl)-L-ornithine (28). To a flask that had been flame-dried and cooled under argon were added 4-cyanomethylimidazole (TCI America, 0.25 g, 2.33 mmol) and anhydrous methanol (10 mL). The solution was cooled on ice, and the HCl gas was bubbled into the solution for 20 min. The reaction mixture was stirred for another 2 h after HCl addition on ice, then the solvent was removed to give a white solid (0.40 g, 2.28 mmol, 98%). The methyl imidic ester was used without further purification. ¹H NMR (500 MHz, D₂O) δ 8.63 (s, 1H), 7.35 (s, 1H), 3.91 (s, 2H), 3.72 (s, 3H).

N^α-Boc-L-Orn-OH (0.75 g, 2.05 mmol), prepared as described above, was dissolved in water (5 mL) and made basic (pH 10) with 2.5 M NaOH. All of the imidic ester was added at once, and the solution was again adjusted to basic pH. After 1 h, the solution was neutralized with 1 M HCl and then left to stir overnight. At that time, the solvent was removed and as much solid residue as possible was dissolved in methanol (3 × 5 mL). The remaining solid was filtered, and the filtrate was concentrated at room temperature. The crude product was purified by ion-exchange chromatography (Bio-Rad 50X, H⁺, 200–400 mesh) and eluted with 3% aqueous pyridine solution to give **28** (0.45 g (1.33 mmol, 65%). ¹H NMR (300 MHz, D₂O) δ 7.70 (s, 1H), 7.10 (s, 1H), 3.90 (m, 1H), 3.81 (s, 2H), 3.00 (t, *J* = 6.9 Hz, 2H), 1.85–1.59 (m, 4H), 1.39 (s, 9H). HRMS (ESI) (*m/z*): M+H⁺ calcd for C₁₀H₁₈N₅O₂ 340.4102, found 340.4105.

5.4.15. N¹-Boc-N⁵-(1-Imino-2-(4-thiophene)ethyl)-L-ornithine (29). 3-Thiopheneacetonitrile (3.0 mL, 26.30 mmol) was converted to the imidic ethyl ester as described above, giving the product (3.15 g (24.46 mmol, 93%) as a brown solid. This was used in the next step without further purification. ¹H NMR (400 MHz, D₂O) δ 7.60 (s, 1H), 7.49 (s, 1H), 7.05 (s, 1H), 4.34 (q, *J* = 6.7 Hz, 2H), 4.05 (s, 2H), 1.42 (t, *J* = 6.5 Hz, 3H).

Coupling with N^α-Boc-L-Orn-OH (0.80 g, 3.44 mmol) was performed with the imidic ester (1.06 g, 5.16 mmol) as described above, except that 1,4-dioxane was used as a co-solvent. All of the solvent was removed, and the residue was re-dissolved in pure water before ion-exchange chromatography to give **29** (0.33 g (0.93 mmol, 27%) as a light-brown solid. ¹H NMR (400 MHz, D₂O) δ 7.50 (s, 1H), 7.38 (s, 1H), 7.07 (d, *J* = 4.80 Hz, 1H), 3.89 (m, 1H), 3.87 (s, 2H), 3.30 (m, 2H), 1.72–1.46 (m, 4H), 1.41 (s, 9H). HRMS (ESI) (*m/z*): M+H⁺ calcd for C₁₆H₂₆N₃O₄S 356.1664, found 356.1656.

5.4.16. *N*⁵-(1-Imino-2-(1-imidazolyl)-ethyl)-L-ornithine (15). Compound **27** (0.20 g, 0.60 mmol) was dissolved in 50% TFA/CH₂Cl₂ (5 mL) and stirred for 1 h, after which time the solvents were removed in vacuo to give **15** in a quantitative yield (0.17 g) as a light yellow solid. A portion of the product was purified by recrystallization from 95% ethanol/ethyl ether. ¹H NMR (500 MHz, D₂O) δ 8.75 (s, 1H), 7.47 (d, 7.0 Hz, 1H), 5.04 (s, 2H), 3.95 (t, *J* = 6.0 Hz, 1H), 3.02 (t, *J* = 8.0 Hz, 2H), 1.99–1.72 (m, 4H). HRMS (ESI) (*m/z*): M+H⁺ calcd for C₁₀H₁₈N₅O₂ 239.2743, found 239.2751.

5.4.17. *N*⁵-(1-Imino-2-(4-imidazolyl)-ethyl)-L-ornithine (16). Compound **28** (126.4 mg, 0.37 mmol) was dissolved in 2 M HCl and stirred for 1 h. The solvent was removed in vacuo to give **16** (115.9 mg, 0.37 mmol). The compound was recrystallized twice from methanol/ethyl ether to give 64.9 mg (56%) of pure compound. ¹H NMR (500 MHz, D₂O) δ 8.75 (s, 1H), 7.45 (s, 1H), 7.46 (s, 1H), 5.04 (s, 2H), 3.95 (t, *J* = 6.0 Hz, 1H), 3.02 (t, *J* = 7.5, 2H), 1.99–1.72 (m, 4H). HRMS (ESI) (*m/z*): M+H⁺ calcd for C₁₀H₁₈N₅O₂ 239.2743, found 239.2738.

5.4.18. *N*⁵-(1-Imino-2-(4-thiophene)-ethyl)-L-ornithine (17). Compound **29** (150.0 mg, 0.42 mmol) was dissolved in 25% TFA/CH₂Cl₂ (5 mL) and stirred for 35 min. The solvent was removed and the residue was re-dissolved in 2 M HCl (3 mL). The solvent was again removed to afford the hydrochloride salt of **17** (140.0 g, 0.41 mmol, 97%). This was recrystallized from ethanol/ethyl ether to give an orange solid in 70% yield. ¹H NMR (500 MHz, D₂O) δ 7.47 (s, 1H), 7.45 (s, 1H), 7.03 (d, *J* = 5.0 Hz, 1H), 4.03 (t, *J* = 6.0 Hz, 1H), 3.85 (s, 2H), 3.32 (t, *J* = 7.0, 2H), 1.97–1.70 (m, 4H). HRMS (ESI) (*m/z*): M+H⁺ calcd for C₁₁H₁₆N₂O₂S 256.1041, found 256.1059.

5.4.19. 2-Methyl-4-thiazolemethanol (30). Ethyl 2-methylthiazole-4-carboxylate was obtained from Alfa Aesar. The ester (1.60 g, 9.27 mmol) was dissolved in dry ethanol (8 mL) and then chilled on ice. To this solution was added a 2 M LiBH₄ solution in THF (11 mL, 22.00 mmol); the solution was allowed to come to room temperature with stirring overnight. After this time, a 1 M citric acid solution (30 mL) was added to quench the reaction. The mixture was then extracted with methylene chloride, the fractions were collected and dried over Na₂SO₄. Pure compound was obtained using silica gel chromatography (1:1 ethyl acetate/hexanes, *R*_f = 0.1), giving **30** (0.78 g, 6.02 mmol, 65%). ¹H NMR (500 MHz, H₂O) δ 6.90 (s, 1H), 5.08 (br s, 1H), 4.56 (s, 2H), 2.52 (s, 3H). HRMS (EI) (*m/z*): M+H⁺ calcd for C₅H₈NOS 129.1802, found 129.1797.

5.4.20. 2-Methyl-4-thiazoleacetonitrile (31). To **30** (0.65 g, 5.07 mmol) was added anhydrous pyridine (0.56 mL, 6.92 mmol). Freshly distilled CH₂Cl₂ (6 mL) was added, and the solution was chilled to –30 °C. Once cool, thionyl chloride (0.68 mL, 9.30 mmol) was added slowly, and after addition, the solution was left to stir for another 2 h while coming to room temperature. By this time, the solution was dark brown. Water (25 mL) was added, and the solution was extracted with CH₂Cl₂. The organic fractions were collected, dried over Na₂SO₄,

and concentrated. To this residue were added sodium cyanide (1.53 g, 31.22 mmol) and DMSO (10 mL). The solution was left to stir overnight. The next morning water (150 mL) was added to the opaque orange solution, and the mixture was extracted with CH₂Cl₂. The organic layers were pooled, dried over Na₂SO₄, and purified by silica gel chromatography (3:2 ethyl acetate/hexanes, *R*_f = 0.57) to obtain **31** (0.21 g, 1.52 mmol, 30%). ¹H NMR (400 MHz, D₂O) δ 7.42 (s, 1H), 4.04 (s, 2H), 2.73 (s, 3H). HRMS (EI) (*m/z*): M+H⁺ calcd for C₆H₇N₂S 139.1902, found 139.1911.

5.4.21. *N*¹-Boc-*N*⁵-(1-Imino-2-(2-methyl-4-thiazole)-ethyl)-L-ornithine (32). Compound **31** (0.17 g, 1.23 mmol) was converted to the methyl imidic ester by dissolving it into anhydrous methanol (10 mL) and bubbling HCl gas through the solution for 20 min. The solvent was removed to give the product as a white solid (0.24 g, 1.16 mmol, 95%). It was used in the next reaction without further purification. ¹H NMR (500 MHz, D₂O) δ 7.70 (s, 1H), 4.06 (s, 2H), 3.76 (s, 3H), 2.94 (s, 2H).

Amidine coupling was performed as described above. *N*²-Boc-L-Orn-OH (0.40 mg, 1.70 mmol), prepared as described above, was allowed to react with the methyl imidic ester (0.23 g, 1.10 mmol). At the completion of the reaction, the water was removed in vacuo, and as much compound as possible was dissolved in methanol (7 mL). The solution was filtered and the filtrate was concentrated without heat. This material was re-dissolved in water, purified by ion-exchange chromatography as before, and eluted with 3% aqueous pyridine solution to give **32** (0.17 mg, 0.46 mmol, 42%). ¹H NMR (400 MHz, CD₃OD) δ 7.29 (s, 1H), 3.95 (m, 1H), 3.68 (s, 2H), 2.19 (t, *J* = 6.8 Hz, 2H), 2.65 (s, 3H), 1.87–1.76 (m, 2H), 1.70–1.67 (m, 2H), 1.41 (s, 9H). HRMS (EI) (*m/z*): M+H⁺ calcd for C₁₆H₂₇N₄O₄S 371.1753, found 371.1760.

5.4.22. *N*⁵-(1-Imino-2-(2-methyl-4-thiazole)-ethyl)-L-ornithine (33). Compound **32** (0.10 g, 0.27 mmol) was dissolved in 2 M HCl (3 mL) and stirred for 45 min. The solvent was removed in vacuo, and the residue was recrystallized from ethanol/ethyl ether to give **33** (32.8 mg, 0.012 mmol, 45%) as a white solid. ¹H NMR (500 MHz, D₂O) δ 7.62 (d, 1H), 4.00 (s, 2H), 3.95 (s, 1H), 3.02 (t, *J* = 7.5 Hz, 2H), 2.70 (s, 3H), 2.03–1.74 (m, 4H). HRMS (EI) (*m/z*): M+H⁺ calcd for C₁₁H₁₉N₄O₄S 271.1237, found 271.1229.

5.5. Enzyme and initial velocity assay

Murine macrophage iNOS was expressed and isolated as previously reported.³⁰ Rat nNOS was expressed and purified according to literature precedent.³¹ Bovine eNOS was isolated by Pavel Martásek at the University of Texas Health Science Center (San Antonio, TX). Nitric oxide production was monitored by the hemoglobin capture assay at 30 °C.³² Briefly, a solution of nNOS or eNOS contained 10 μM L-arginine, 1.6 mM CaCl₂, 11.6 μg/mL calmodulin, 100 μM DTT, 100 μM NADPH, 6.5 μM H₄B, 3 mM oxyhemoglobin, and specified inhibitor concentration in 100 mM Hepes (pH 7.5) in 600 μL total volume; iNOS contained the same con-

centrations of cofactors, except CaCl_2 and calmodulin were not included. The assay was initiated by addition of enzyme and monitored at 401 nm on a Perkin-Elmer Lambda 10 UV-vis spectrophotometer.

5.6. K_i value determination

The K_i values were obtained following the method of Dixon.³³ The initial reaction velocity was measured using at least four different inhibitor concentrations at four different substrate concentrations: 10 μM , 6 μM , 3 μM , and 1 μM . The measurements for each substrate concentration were plotted as a line, with the deviation from the mean of the measurements being less than $\pm 5\%$. These lines were then plotted on the same graph, and points of intersection within $\pm 7\%$ of the mean were used to give the average to give the mean K_i .

5.7. Difference spectra

Inhibitor perturbation difference spectrophotometry measurements of nNOS were performed according to the procedure of Fast and Silverman.^{18a} A solution of 1.55 μM nNOS in a solution of 10 μM H_4B , 10% glycerol, and 100 mM Hepes (pH 7.5) was scanned against a blank solution without nNOS from 375 to 475 nm. Imidazole (1 mM) was added, and the solution was scanned again. For compounds **9**, **10**, and **14** a 6.0 mM inhibitor solution was added in 2 μL aliquots over four scans (many times this led to saturation, and no difference was seen after the second or third addition). For compounds **11** and **12**, an inhibitor solution of 60 mM was used. The nNOS/imidazole spectrum was then subtracted from each of these, the plots normalized to 0.001 at 430 nm and smoothed to obtain the spectra. The total volume of aliquots did not exceed 5% of the total volume. The same procedure was used for testing compound **15** against iNOS.

5.8. Irreversible inhibition kinetics

nNOS was incubated at 0 °C in Hepes buffer (100 mM, pH 7.5) containing catalase (1000 U), NADPH (9 μM), H_4B (1 μM), dithiothreitol (10 μM), glycerol (10% v/v), and inactivator in a total volume of 140 μL . The reactions were initiated by the addition of enzyme, and 10 μL aliquots were removed at specified time points and tested via the initial velocity assay. Controls were performed by replacing inhibitor volume with Hepes buffer or replacing NADPH with NADP^+ . Inactivation studies with compound **15** and iNOS were conducted similarly, except for temperature differences as noted. K_i and k_{inact} values were determined by the method of Kitz and Wilson.³⁴

5.9. Activity recovery determination

An incubation mixture of nNOS with compound **9** (25 μM) and a control were prepared as described above and kept at 0 °C. After the incubation containing **9** showed no activity (2.75 h), an L-arginine solution (6 mM) was added to both incubations to bring the substrate concentration to 250 μM . The solution volume

was altered less than 4%. Initial velocity assays were performed with each incubation every 10 min for 1 h to monitor the change in activity.

5.10. HPLC of products formed from inactivation of nNOS by **9**

Chromatograms of biliverdin IX α , hemin, and the incubation mixtures were obtained on a C18 reversed-phase column (Vydac, 218TP54, 5 μm , 4.6 \times 250 mm) at 401 nm with 60% H_2O (0.1% TFA) and 40% CH_3CN (0.1% TFA) with a flow rate of 1.0 mL/min. The incubation mixtures were prepared as above with the control prepared by substituting **9** with Hepes buffer. Injections were made immediately after the addition of nNOS to the incubation mixture and after the incubation containing **9** no longer showed any activity (4.5 h). A standard curve was also generated to correlate the biliverdin IX α concentration to the area under the curve by obtaining four chromatographs of biliverdin IX α with concentrations ranging from 60 μM to 0.06 μM in solutions of 30% DMSO/ H_2O .

Acknowledgments

We are grateful to the National Institutes of Health (GM 49725 to R.B.S. and GM52419 and HL30050 to Prof. Bettie Sue Masters, in whose laboratory P.M. and L.J.R. work) for financial support of this work.

Supplementary data

Supplementary data associated with this article can be found, in the online version, at [doi:10.1016/j.bmc.2005.12.043](https://doi.org/10.1016/j.bmc.2005.12.043).

References and notes

1. Kerwin, J. F., Jr.; Lancaster, J. R., Jr. *Med. Res. Rev.* **1994**, *14*, 23–74.
2. MacMicking, J.; Xie, Q. W.; Nathan, C. *Annu. Rev. Immunol.* **1997**, *15*, 323–350.
3. Rapoport, R. M.; Murad, F. J. *Cyclic Nucl. Prot.* **1983**, *9*, 281–290.
4. Schmidt, H. H. H. W.; Walter, U. *Cell* **1994**, *78*, 919–925.
5. (a) Mayer, B.; Hemmens, B. *Trends Biochem. Sci.* **1997**, *22*, 477–481; (b) Dawson, V. L.; Dawson, T. M.; London, E. D.; Bredt, D. S.; Snyder, S. H. *Proc. Natl. Acad. Sci. U.S.A.* **1991**, *88*, 6368–6371.
6. Choi, D. W.; Rothman, S. M. *Annu. Rev. Neurosci.* **1990**, *13*, 171–182.
7. MacIntyre, I.; Zaidi, M.; Alam, A. S.; Datta, H. K.; Moonga, B. S.; Lidbury, P. S.; Hecker, M.; Vane, J. R. *Proc. Natl. Acad. Sci. U.S.A.* **1991**, *88*, 2936–2940.
8. Frey, C.; Narayanan, K.; McMillan, K.; Spack, L.; Gross, S. S.; Masters, B. S.; Griffith, O. W. *J. Biol. Chem.* **1994**, *269*, 26083–26091.
9. Crane, B. R.; Arvai, A. S.; Ghosh, D. K.; Wu, C.; Getzoff, E. D.; Stuehr, D. J.; Tainer, J. A. *Science* **1998**, *279*, 2121–2126.
10. (a) Cramer, S. P.; Dawson, D. H.; Hodgson, K. O.; Hager, L. P. *J. Am. Chem. Soc.* **1978**, *100*, 7282–7290; (b) Tang, S.

- C.; Koch, S.; Papaefthymiou, G. C.; Foner, S.; Frankel, R. B.; Ibers, J. A.; Holm, R. H. *J. Am. Chem. Soc.* **1976**, *98*, 2414–2434.
11. Lee, Y.; Martasek, P.; Roman, L. J.; Masters, B. S. S.; Silverman, R. B. *Bioorg. Med. Chem.* **1999**, *7*, 1941–1951.
12. Wolff, D. J.; Datto, G. A.; Samatovicz, R. A.; Tempside, R. A. *J. Biol. Chem.* **1993**, *168*, 9425–9429.
13. (a) Babu, B. R.; Frey, C.; Griffith, O. W. *J. Biol. Chem.* **1999**, *274*, 25218–25226; (b) Gachhui, R.; Ghosh, D. K.; Chaoqun, W.; Parkinson, J.; Crane, B. R.; Stuehr, D. J. *Biochemistry* **1997**, *36*, 5097–5103.
14. Rarey, M.; Wefing, S.; Lengauer, T. *J. Comput. Aid. Mol. Des.* **1996**, *10*, 41–54.
15. Fazio, O.; Gnida, M.; Meyer-Klaucke, W.; Frank, W.; Klau, W. *Eur. J. Inorg. Chem.* **2002**, *11*, 2891–2896.
16. Berka, V.; Chen, P.-F.; Tsai, A.-L. *J. Biol. Chem.* **1996**, *271*, 33293–33300.
17. Pinner, A.; Klein, F. *Umwandlung der Nitrile in Imide. Ber.* **1877**, *10*, 1889–1897.
18. (a) Fast, W.; Nikolic, D.; Van Breemen, R. B.; Silverman, R. B. *J. Am. Chem. Soc.* **1999**, *121*, 903–916; (b) Moore, W. M.; Webber, R. K.; Jerome, G. M.; Tjoeng, F. S.; Misko, T. P.; Currie, M. G. *J. Med. Chem.* **1994**, *37*, 3886–3888.
19. Van Bogaert, I.; Haemers, A.; Bollaert, W.; Van Meirvenne, N.; Brun, R.; Smith, K.; Fairlamb, A. H. *Eur. J. Med. Chem.* **1993**, *28*, 387–397.
20. Zhu, Y.; Nikolic, D.; Van Breeman, R. B.; Silverman, R. B. *J. Am. Chem. Soc.* **2004**, *127*, 858–868.
21. Zhang, H. Q.; Fast, W.; Marletta, M. A.; Martasek, P.; Silverman, R. B. *J. Med. Chem.* **1997**, *40*, 3869–3870.
22. Babu, B. R.; Griffith, O. W. *J. Biol. Chem.* **1998**, *273*, 8882–8889.
23. Zhang, H. Q.; Dixon, R. P.; Marletta, M. A.; Nikolic, D.; Van Breeman, R.; Silverman, R. B. *J. Am. Chem. Soc.* **1997**, *119*, 10888–10902.
24. Li, H.; Raman, C. S.; Martasek, P.; Král, V.; Masters, B. S. S.; Poulos, T. L. *J. Inorg. Biochem.* **2000**, *81*, 133–139.
25. Fedorov, R.; Hartmann, E.; Ghosh, D. K.; Schlichting, I. *J. Biol. Chem.* **2003**, *278*, 45818–45825.
26. Barker, P. L.; Gendler, P. L.; Rapoport, H. *J. Org. Chem.* **1981**, *26*, 2455–2465.
27. Takeda, K.; Akiyama, A.; Nakamura, H.; Takizawa, S.; Mizuno, Y.; Takayanagi, H.; Harigaya, Y. *Synthesis* **1994**, *10*, 1063–1066.
28. Johnston, T. P.; Gallagher, A. *J. Org. Chem.* **1963**, *28*, 1436–1437.
29. de la Hoz, A.; Blasco, H.; Diaz-Ortiz, A.; Elguero, J.; Concepcion, F.-F.; Moreno, A.; Sanchez-Migallon, A.; Valiente, G. *New J. Chem.* **2002**, *7*, 926–932.
30. Hevel, J. M.; White, K. A.; Marletta, M. *J. Biol. Chem.* **1991**, *266*, 22789–22791.
31. (a) Roman, L. J.; Sheta, E. A.; Martasek, P.; Gross, S. S.; Liu, Q.; Masters, B. S. S. *Proc. Natl. Acad. Sci. U.S.A.* **1995**, *92*, 8428–8432; (b) Gerber, N. C.; Montelloano, P. R. *J. Biol. Chem.* **1995**, *270*, 17991–17996.
32. Hevel, J. M.; Marletta, M. *Methods Enzymol.* **1994**, *133*, 250–258.
33. Dixon, M. *Biochem. J.* **1953**, *55*, 170.
34. Kitz, R.; Wilson, I. B. *J. Biol. Chem.* **1962**, *237*, 3245–3249.